arXiv:astro-ph/9809040v1 3 Sep 1998

NICMOS and WFPC2 Imaging of Ultraluminous Galaxies

K. D. Borne

Raytheon STX Corporation, NASA Goddard Space Flight Center

H.Bushouse, L.Colina, R.A.Lucas, A.Baker, D.Clements, A.Lawrence, S.Oliver, & M.Rowan-Robinson

Abstract. HST is used to study the power sources and the interaction-induced tidal disturbances within the most luminous galaxies in the local universe — the Ultra-Luminous IR Galaxies (ULIRGs) — through the use of I-band images with WFPC2 and H-band images with NICMOS.

1. Introduction to Interactive Galaxies and ULIRGs

Ultraluminous IR galaxies (ULIRGs; with luminosities [8–1000μm] in excess of $10^{12} L_{\odot}$) are the most luminous galaxies in the local universe. They are believed to be powered by massive bursts of star formation that are induced by violent galaxy-galaxy collisions (Genzel et al. 1998). This "interaction-activity connection" and the corresponding physical processes seen in ULIRGs locally are believed to have been more prevalent at high redshift – thus perhaps explaining the quasar phenomenon and maybe even galaxy formation itself (Sanders & Mirabel 1996; and references therein). We are obtaining high-resolution images of ULIRGs with the Hubble Space Telescope (HST). Such images are probing for the first time the fine-scale structure in the strong collision-disturbed morphologies of these rare and exotic galaxies (Borne et al. 1997a,b,c,d). The significance of ULIRGs is underscored by their relevance to galaxy formation, star formation, galaxy evolution, and the IR background, as evidenced by their prominence within the overall science missions of ISO, WIRE, SIRTF, and NGST (e.g., Bushouse et al. 1997). Their significance has been further highlighted recently by the apparent resolution of ∼30-50% of the IR background in the submillimeter with SCUBA and the subsequent identification of those sources with high-redshift ULIRGs (Hughes et al. 1998; Barger et al. 1998).

2. HST Observations and Results

We are carrying out a thorough survey and analysis of HST imaging data on ULIRGs, including nearly 120 I-band and over 30 H-band images. All our observations were obtained as part of HST snapshot survey programs. We selected objects from the bright samples of Sanders et al. (1988a,b) and Melnick & Mirabel (1990), and from the QDOT sample (Leech et al. 1994; Lawrence et al., in press). The WFPC2 images were obtained with the I-band filter (F814W at 8000A), with galaxies typically centered in the WF3 chip (800x800 pixels,

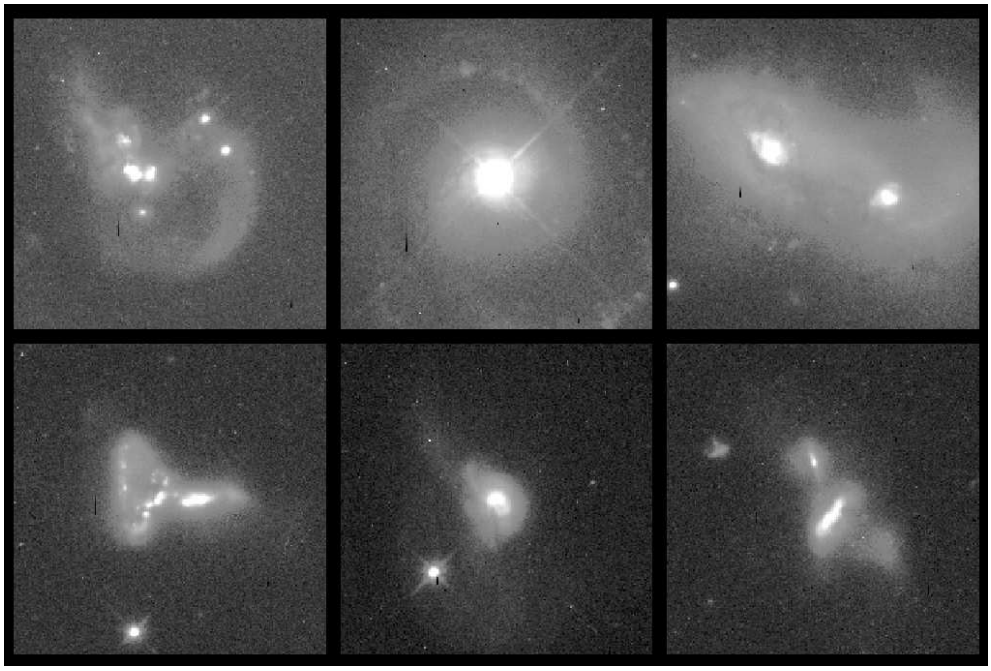

Figure 1. Representative WFPC2 images (see text for details).

at 0.1″/pixel). The NICMOS exposures were obtained with the H-band filter (F160W at 1.6μm). The images were spiral-dithered in 'multiaccum' mode, with galaxies centered in the NIC2 camera FOV (256x256 pixels, at 0.075″/pixel).

2.1. WFPC2 Results

We show representative results from our WFPC2 imaging sample in Figure 1. Each of the 120 ULIRGs that we have imaged with WFPC2 falls into one of the classes that are represented by these six examples. *Top Left* – In nearly all ULIRGs, massive star formation is seen on all scales in the HST images, including super star clusters of the type seen in HST images of other colliding galaxies, indicating that a giant starburst is the dominant power source in most ULIRGs. *Top Middle* – A star–like nucleus is seen in 10% of the ULIRGs, for which the dominant power source may be a dust–enshrouded AGN/QSO. *Top Right* – Several of the galaxies show clear evidence in HST images for a ring around the central nucleus, very similar to rings seen in HST images around the centers of other 'black hole'–powered galaxies. *Lower Left* – There is evidence for at least one classical collisional ring galaxy in the sample, similar to the Cartwheel ring galaxy imaged by us with HST. *Lower Middle* – Some ULIRGs previously classified as non-interacting from ground-based images now show in HST images clear evidence of merging (a second nucleus) or of interaction (e.g., tidal tails). *Lower Right* – Many ULIRGs appear to have physically associated companions, perhaps related to the collision, merger, and subsequent starburst.

Figure 2. HST comparison images of IR11095-0238. Left: NICMOS H-band image. Right: WFPC2 I-band image. (See text for details.)

2.2. NICMOS-WFPC2 Intercomparisons

We are using our multiple-waveband data set to derive wavelength dependencies in the morphologies of ULIRGs, hence measuring the spatial variations and effects of dust, star formation, and stellar population within these highly disturbed galaxies. We present some preliminary comparisons between the NICMOS and WFPC2 images here for several ULIRGs (listed in Table 1). A representative example (IR11095-0238) is displayed in Figure 2.

Table 1. Subsample of ULIRGs for NIC–WF Intercomparisons.

Target Name	Redshift	F(60μm)	$\log L_{IR}/L_{\odot}$	AGN ?
IR11095-0238 (*Fig. 2*)	0.1066	3.2 Jy	12.15	Liner
IR23128-5919	0.0446	10.8 Jy	11.95	SB + Sey 2(?)
QDOT044123+260833	0.1712	0.8 Jy	12.16	Sey 2
QDOT052321-233443	0.1717	0.5 Jy	12.16	Sey 2
QDOT062652+350957	0.1698	0.9 Jy	12.22	
QDOT105551+384511	0.2066	0.6 Jy	12.07	
QDOT200342-154747	0.1919	1.6 Jy	12.59	Sey 1

IR11095-0238 : (Displayed in Figure 2.) Significant dust, star-forming knots, and tidal features are seen in the WF image. Simple double-galaxy morphology is seen in NIC image, with little dust mottling and weak tidal features. Two faint knots parallel to and just to the right of the two nuclei are seen in both images.

IR23128-5919 : Many knots, small-scale features, and large-scale features (probably tidal in origin) are seen in both the NIC and the WF images. The appearance of the galaxies in the WF image is strongly affected by dust obscuration, some of which is also seen in the NIC image.

QDOT044123+260833 : NIC image shows brighter more compact nucleus. WF image shows sharper spiral arms, and possibly knots. The central bar is more prominent in the NIC image.

QDOT052321-233443 : WF image shows slightly more extended nucleus. Tidal arm(s) are visible in both, but very weak in NIC image. Tidal arm seen clearly in WF image of companion.

QDOT062652+350957 : Similar appearance in both images, though higher S/N in WF allows for more features to be seen. Some possible star-forming knots (tidal dwarf galaxies?) are seen clearly in WF image of tidal tails.

QDOT105551+384511 : Very different appearance between NIC and WF. Position angle between two major nuclei differs in the two images. Much greater tidal extensions are seen in the WF image (possible S/N effect).

QDOT200342-154747 : Seyfert 1 nucleus dominates, especially in NIC image. Much more structure seen in WF image: in the "companion" and in the surrounding tidal debris. Possibly multiple companions are seen in the WF image — may be tidal dwarf galaxies in formation.

Acknowledgments. Support for this work was provided by NASA through grant numbers GO–6346.01–95A and GO–7896.01–96A from the Space Telescope Science Institute, which is operated by AURA, Inc., under NASA contract NAS5–26555.

References

Barger, A. J., et al. 1998, Nature, 394, 241

Borne, K., et al. 1997a, in IAU Symposium 179: New Horizons from Multi-Wavelength Sky Surveys, B. McLean et al., Dordrecht: Kluwer, 275

Borne, K., et al. 1997b, in Star Formation, Near and Far, S. Holt & L. Mundy, Woodbury: AIP, 295

Borne, K., et al. 1997c, in Extragalactic Astronomy in the Infrared, G. A. Mamon et al., Paris: Editions Frontieres, 277

Borne, K., et al. 1997d, in The Ultraviolet Universe at Low and High Redshift , eds. W. H. Waller et al., Woodbury: AIP, 423

Bushouse, H., et al. 1997, in Science with the Next Generation Space Telescope, E. P. Smith & A. Koratkar, San Francisco: ASP, 233

Genzel, R., et al. 1998, ApJ, 498, 579

Hughes, D. H., et al. 1998, Nature, 394, 248

Leech, K. J., et al. 1994, MNRAS, 267, 253

Melnick, J., & Mirabel, I. F. 1990, A&A, 231, L19

Sanders, D. B., et al. 1988a, ApJ, 325, 74

Sanders, D. B., et al. 1988b, ApJ, 328, L35

Sanders, D. B., & Mirabel, I. F. 1996, ARA&A, 34, 749